jove

Double Direct Injection of Blood into the Cisterna Magna as a Model of Subarachnoid Hemorrhage

Martin Pedard[1], **Mohamad El Amki**[1], **Antoine Lefevre-Scelles**[1,2], **Vincent Compère**[1,2], **Hélène Castel**[1]

[1] University of Rouen Normandy, INSERM U1239, DC2N, Institute for Research and Innovation in Biomedicine (IRIB), Rouen, France [2] Department of Anesthesiology and Critical Care, Rouen University Hospital, Rouen, France

Corresponding Author

Hélène Castel
helene.castel@univ-rouen.fr

Citation

Pedard, M., El Amki, M., Lefevre-Scelles, A., Compère, V., Castel, H. Double Direct Injection of Blood into the Cisterna Magna as a Model of Subarachnoid Hemorrhage. *J. Vis. Exp.* (162), e61322, doi:10.3791/61322 (2020).

Date Published

August 30, 2020

DOI

10.3791/61322

URL

jove.com/video/61322

Abstract

Among strokes, subarachnoid hemorrhage (SAH) consecutive to the rupture of a cerebral arterial aneurysm represents 5-9% but is responsible for about 30% of the total stroke-related mortality with an important morbidity in terms of neurological outcome. A delayed cerebral vasospasm (CVS) may occur most often in association with a delayed cerebral ischemia. Different animal models of SAH are now being used including endovascular perforation and direct injection of blood into the cisterna magna or even the prechiasmatic cistern, each exhibiting distinct advantages and disadvantages. In this article, a standardized mouse model of SAH by double direct injection of determined volumes of autologous whole blood into the cisterna magna is presented. Briefly, mice were weighed and then anesthetized by isoflurane inhalation. Then, the animal was placed in a reclining position on a heated blanket maintaining a rectal temperature of 37 °C and positioned in a stereotactic frame with a cervical bend of about 30°. Once in place, the tip of an elongated glass micropipette filled with the homologous arterial blood taken from carotid artery of another mouse of the same age and gender (C57Bl/6J) was positioned at a right angle in contact with the atlanto-occipital membrane by means of a micromanipulator. Then 60 µL of blood was injected in the cisterna magna followed by a 30° downward tilt of the animal for 2 minutes. The second infusion of 30 µL of blood into the cisterna magna was performed 24 h after the first one. The individual follow-up of each animal is carried out daily (careful evaluation of weight and well-being). This procedure allows a predictable and highly reproducible distribution of blood, likely accompanied by intracranial pressure elevation that can be mimicked by an equivalent injection of an artificial cerebral spinal fluid (CSF), and represents an acute to mild-model of SAH inducing low mortality.

Introduction

Subarachnoid hemorrhage (SAH) accounts for up to 5% of all stroke cases and constitutes a relatively common pathology with an incidence of 7.2 to 9 patients per 100,000 per year, with a mortality rate of 20%-60% depending on the study[1,2,3]. In the acute phase, the mortality is attributable to the severity of bleeding, rebleeding, cerebral vasospasm (CVS) and/or medical complications[4]. In survivors, early brain injury (EBI) is associated with parenchymal extension of hemorrhage and abrupt increase in intracranial pressure, which may result in primary cerebral ischemia[5] and immediate death in about 10%-15% of cases[6]. After the initial "acute" stage of SAH, the prognosis depends on the occurrence of "secondary" or delayed cerebral ischemia (DCI), detected in nearly 40% of patients by cerebral computed tomography, and in up to 80% of patients after magnetic resonance imaging (MRI)[7,8]. In addition to the CVS occurring between 4 to 21 days after aneurysm rupture in a majority of SAH patients, DCI[9] may result from multifactorial diffuse brain lesions secondary to microthrombosis formation, reduced cerebral perfusion, neuroinflammation, and cortical spreading depression (CSD)[10,11,12,13]. This affects 30% of SAH survivors and impacts cognitive functions including visual memory, verbal memory, reaction time, and executive, visuospatial and language functions[14] impairing daily life[15]. Current standard therapies to prevent CVS and/or the poor cognitive outcomes in SAH patients are based on the blockage of Ca^{2+} signaling and vasoconstriction by using Ca^{2+} channel inhibitors as Nimodipine. However, more recent clinical trials targeting vasoconstriction revealed dissociation between patient's neurological outcome and prevention of CVS[16], suggesting more complex pathophysiological mechanisms involved in SAH-long-term consequences. Therefore, there is a medical need for greater understanding of the number of pathological events accompanying SAH and the development of valid and standardized animal models to test original therapeutic interventions.

The rupture of an intracranial aneurysm mostly responsible for SAH in humans is likely difficult to mimic in preclinical animal models. Currently, the aneurysm rupture and SAH situation can tentatively be tested by the perforation of the middle cerebral artery (endovascular puncture model) responsible for CVS and sensitivomotor dysfunctions in mice[17,18]. Due to the lack of any possible control over the onset of bleeding and the diffusion of blood in this model, other methods have been developed in rodents to generate SAH models without endovascular rupture. More precisely, they consist of the direct administration of arterial blood into the subarachnoid space through a single or a double injection in the magna cisterna[19] or a single injection into the prechiasmatic cistern[20]. The main advantage of these mouse models without endovascular rupture is the possibility to reproducibly master the surgical procedure and the quality and quantity of the injected blood sample. Another advantage of this model over the model by endovascular perforation in particular is the preservation of the general well-being of the animal. As a matter of fact, this surgery is less invasive and technically less challenging than that required to generate a carotid wall rupture. In this last model, the animal has to be intubated and mechanically ventilated, while a monofilament is inserted in the external carotid artery, and advanced into the internal carotid artery. This likely leads to transient ischemia due to vessel obstruction by the wire path. Consequently, the co-morbidity (moribund state, important pain and death) associated with surgery is less important in double injection model compared with endovascular perforation model. In

addition to being a more consistent SAH, the double direct injection method complies with the animal welfare in research and testing (reduced time under anesthesia, pain from tissue disruption in surgery and distress) and leads to a minimum total number of animals used for the protocol study and personnel training.

Moreover, this allows implementation of the same protocol to transgenic mice, leading to an optimized pathological understanding of the SAH and the possibility of comparative testing of potential therapeutic compounds. Here, we present a standardized mouse model of subarachnoid hemorrhage (SAH) by a double daily consecutive injection of autologous arterial blood into the cisterna magna in 6-8 weeks-old male C57Bl/6J mice. The main advantage of this model is the control of the bleeding volume compared with the endovascular perforation model, and the reinforcing of the bleeding event without a drastic increase of intracranial pressure[21]. Recently, the double direct injection of blood into the cisterna magna has been well described on the experimental and physiopathological issues in mice. Indeed, we recently demonstrated CVS of large cerebral arteries (basilar (BA), middle (MCA) and anterior (ACA) cerebral arteries), cerebrovascular fibrin deposition and cell apoptosis from day 3 (D3) to 10 (D10), circulation defects of paravascular cerebrospinal fluid accompanied by altered sensitivomotor and cognitive functions in mice, 10 days post-SAH in this model[22]. Thus, it makes this model mastered, validated and characterized for short-term and long-lasting events post-SAH. It should be ideally suitable for prospective identification of new targets and for studies on potent and efficient therapeutic strategies against SAH-associated complications.

Protocol

All procedures were performed under the supervision of H. Castel in accordance with the French Ethical Committee and guidelines of European Parliament Directive 2010/63/EU and the Council for the Protection of Animals Used for Scientific Purposes. This project was approved by the local CENOMEXA and the national ethic committees on animal research and testing. Male C57Bl/6J Rj mice (Janvier), aged 8–12 weeks, were housed under controlled standard environmental conditions: 22 °C ± 1 °C, 12 hours/12 hours light/dark cycle, and water and food available ad libitum.

1. Setup of SAH surgery and preparation for injection

1. Before the beginning of surgery, pull an adequate number of glass capillaries by using a micropipette puller. The injection pipette should exhibit an inner diameter of 0.86 mm and outer diameter of 1.5 mm.
2. Prepare the artificial cerebrospinal fluid (aCSF) for the sham condition.
    1. Prepare a solution with 119 mM NaCl, 2.5 mM KCl, 1 mM NaH_2PO_4, 1.3 mM $MgCl_2$, 10 mM glucose, 26.2 mM $NaHCO_3$ in H_2O, pH 7.4.
    2. Gas aCSF with 95% O_2 and 5% CO_2 for 15 min, and then add 2.5 mM $CaCl_2$.
    3. Sterilize the oxygenated aCSF with a 0.22 µm filter apparatus. The aCSF solution can be stable for 3-4 weeks at 4 °C. If contamination (solution becoming cloudy) or a deposit formation has appeared, discard and make fresh aCSF.
3. Collection of blood from a homologous mouse donor

1. Isolate the carotid artery along the trachea and collect the maximum amount of blood by puncture of the carotid artery.
2. In practice, place the mouse into an anesthesia chamber and load the chamber with 5% isoflurane until the animal loses consciousness.
3. Check the lack of reflexes by clamping one of two hind limbs to allow the setting of the surgical experimental procedure.
4. Coat a 1 mL syringe with a heparin solution by using a 26 G needle (heparin sodium). This will prevent blood coagulation during the next steps.
5. Install the animal positioned in dorsal decubitus with legs apart, and the nose in an anesthesia mask (anesthesia maintenance with 2 to 2.5% isoflurane).
6. Isolate the carotid artery along the trachea by dissecting the omohyoid muscle longitudinally. Once artery isolated, insert the needle towards the heart with the help of the microdissecting hook and forceps and collect the maximum of blood via puncture of the carotid artery (60 µL is needed per SAH mouse).
7. Sacrifice the anesthetized donor mouse immediately after blood collection by using cervical dislocation.

2. Animal (8-10-week-old C57BL/6J male mice) preparation

1. Weigh each mouse precisely using an electronic balance. In the current study, mice would have body weight within the range of 20 to 25 grams just before surgery.
2. As previously explained (see steps 1.3.2 and 1.3.3), induce anesthesia of mice to be operated.
3. Shave the neck and the space between the ears with a suitable electric clipper.
4. Install the animal positioned in ventral decubitus with legs apart and the nose in an anesthesia mask (anesthesia maintenance with 2 and 2.5% isoflurane) on a stereotactic frame.
5. Check that the mouse is sleeping and that his head is properly blocked.
6. Subcutaneously inject 100 µL of buprenorphine (0.1 mg/kg) with a 26 G needle in the lower back, to avoid pain after awakening.
7. Prevent dry eyes by using protective liquid gel and maintain an intrarectal temperature of 37 °C by using an auto-regulated electric blanket.
8. Treat the posterior neck shaved area with an antiseptic solution (povidone-iodine or chlorhexidine by using a sterile cotton road).
9. Pre-sterilize all instruments touching the prepared skin/subcutaneous tissue (heating to 200 °C for 2 hours) and handle aseptically.

3. SAH induction

1. On the first day (D-1)
    1. Cut a 1 cm incision with thin scissors in the posterior neck, followed by the separation of muscles along the midline to access the cisterna magna.
    2. Cut the tip of the empty glass pipette with thin scissors. Then, adapt to a syringe connected to a flexible silicone connector.
    3. Transfer 60 µL of blood or aCSF (for SAH or sham condition, respectively) in a 0.5 mL tube using a precision micropipette.

4. Suck into the glass pipette the 60 µL of blood for the SAH condition or 60 µL of aCSF for the sham condition.
5. For injection, install the pipette on the stereotactic frame using a ring or blue-tack and slowly bring the pipette tip to the membrane at the interface with the cisterna magna.
6. Slowly insert the pipette tip through the atlanto-occipital membrane into the cisterna magna, using a micro-manipulator of the stereotactic frame.
7. Connect the pipette previously filled with blood or aCSF to the syringe ready for pressure induction.
8. Inject by pressing the plunger at a low rate around 10 µL/min, to avoid acute intracranial pressure.
9. During injection, closely monitor the respiratory rate and the rectal temperature.
10. At the end of the injection, carefully take off the pipette via the micro-manipulator and visually ensure that there is no leak during withdrawal.
11. Achieve hemostasis using an absorbable hemostat and run two sutures with braided non-absorbable suturing thread.
12. Immediately after surgery, isolate and position the mouse in decline decubitus and cover it with a survival blanket in an open box for the duration of recovery.

2. Second day of induction (D0)
    1. After 24 hours, induce anesthesia (see steps 1.3.2 and 1.3.3). Subcutaneously inject 100 µL of buprenorphine again (0.1 mg/kg) and prevent dry eyes by using protective liquid gel (see steps 2.7 and 2.8).
    2. Install the animal on the stereotactic frame as the day before.
    3. Carefully remove the sutures with microscissors.
    4. Prepare the atlanto-occipital membrane as before and apply antiseptic preparation on the shaved area of the neck with a sterile cotton rod.
    5. Inject 30 µL of blood or aCSF at a low rate (see steps 3.1.2 to 3.1.8). Monitor the respiratory rate and the rectal temperature.
    6. At the end of the injection, carefully take off the pipette and control the absence of blood leak during withdrawal.
    7. Achieve hemostasis and run two sutures with braided absorbable suturing thread.

4. Postoperative follow-up and end of the experiment

1. Immediately after surgery, isolate and position the mouse in decline decubitus with a survival blanket on its back in an open box during recovery.
2. Weigh and carefully observe daily the behavior of each mouse until sacrifice (e.g., D7 post-surgery).
3. Among humane endpoints, a significant weight loss (>15% of the weight) is classically noticed. A "hunched back" posture, slow movements, prostration, abnormal vocalizations of hurt and/or significant aggressive behavior are also important signs of animal suffering. If any of these signs or a combination of signs appears, the monitoring of the animal is reinforced within hours of their appearance. If the animal's welfare worsens or does not improve within 48 hours, it will be considered that a level of intolerable suffering is reached, and euthanasia is carried out.

4. At the time of choice, sacrifice anesthetized mice by decapitation, and harvest brains for further analyses.
5. Perform euthanasia (decapitation) after isoflurane anesthesia (5%).

Representative Results

Experimental timeline, procedure, follow-up and mortality

Figure 1A and **Figure 1B** summarize the SAH model protocol by double intracisternal injection of blood. Briefly, on the first day of SAH induction (D-1), 60 µL of blood withdrawn from a homologous mouse or 60 µL of artificial cerebrospinal fluid (aCSF) were injected into the cisterna magna in SAH or sham conditions, respectively. The next day (D0), 30 µL of blood withdrawn from a homologous mouse or 30 µL of aCSF were injected into the cisterna magna in SAH or Sham conditions, respectively. Twenty-four hours after surgery, mouse killing and brain analysis allowed to observe the blood distribution into the paravascular spaces as illustrated in **Figure 1C**. As a sensitive indicator for general welfare from D1 to sacrifice, the body weight was daily assessed from the D1 to D8 and showed a significant reduced body weight gain in SAH compared with sham animals from D1 to D8 (**Figure 1D**), suggesting a long-lasting recovery process and prolonged pathological events post-SAH. Post-operative mortality was 26.7% at D7 with most animals dying on D1 or D4 after surgery (**Figure 1D**). Transcardial perfusion of Indian ink at D5 enabled the observation of macroscopic CVS as illustrated in **Figure 1C**.

Cerebral vasospasm after SAH

As shown by El Amki et al.[22], CVS of the basilar artery (BA), middle cerebral artery (MCA) and anterior cerebral artery (ACA) was present in SAH model by double intracisternal injection of blood in either ACA, MCA or BA from D3 to D10 post-surgery. Briefly (**Figure 2A**), after mouse sacrifice and decapitation, brains were harvested and post-fixed in 4% paraformaldehyde (PFA), and then frozen at -80 °C, before being sliced into 20 µm transversal slices using a cryostat. Hematoxylin and eosin staining was performed for BA (interaural 0.40 mm; bregma -3.40 mm), MCA (interaural 2.58 mm; bregma -1.22 mm) and ACA (interaural 4.90 mm; bregma 1.10 mm) to allow CVS identification via systematic image acquisition of colored slices by using a microscope-mounted camera. In order to evaluate the absence or the presence of macroscopic CVS, the lumen area/wall thickness ratio was calculated for each stained artery. The lower is the ratio, the more severe is the CVS. Thus, a CVS occurred in BA in SAH brains compared with sham mouse brains (**Figure 2B**) but also in other large cerebral arteries (MCA, ACA, data not shown[22]).

Sensitivomotor dysfunctions after SAH

The measurement of specific motor deficits, well described in this SAH model by El Amki et al.[22] and Clavier et al.[23], can be considered as a main evaluation criterion of outcome to test specific therapeutic targets regulating these SAH-associated long-term effects. Briefly (**Figure 3A**), at D6 post-surgery, each mouse was evaluated in the open-field test for 10 minutes. By means of the ANY-maze software version 4.99, the distance covered and the number of rearing and leaning were recorded. Twenty-four hours after the open-field test, each mouse took part in three successive sessions of the beam walking test involving, after a device habituation period, the measurement of total walking time, the time to reach the platform and the number of trips. Results were expressed as a mean of three sessions. As shown by El Amki et al.[22], sensitivomotor dysfunctions evaluated by the beam walking test at D10 post-surgery were shown to be present in the SAH model (**Figure 3B**). At D9, spontaneous activity

of mice evaluated by the open-field test during 10 minutes, was also significantly affected by SAH as detected by the distance crossed and the vertical activity compared with the sham condition (**Figure 3C**).

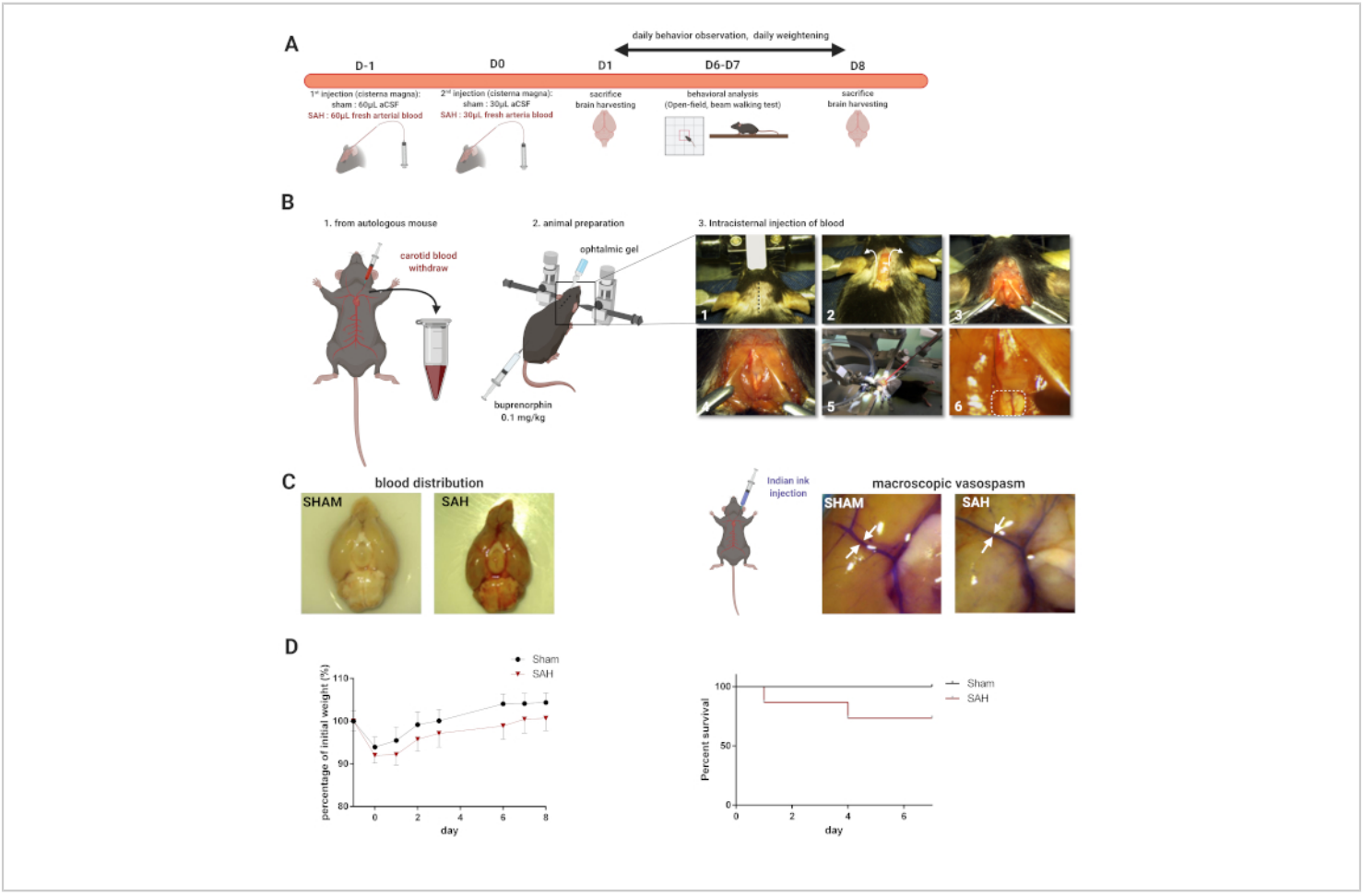

Figure 1. Experimental design, surgical procedure, blood distribution, macroscopic vasospasm, body weight and mortality after SAH. (**A**) Schematic diagram showing the experimental design of this protocol. D-1 and D0 represent the days of surgery with a double injection of 60 and 30 µL of aCSF (Sham) or blood (SAH) into the cisterna magna, respectively. From D1 to D8, mice were daily observed and weighed. At D1, brains were harvested to observe the blood distribution into paravascular spaces (**C**). The D6 and D7 were chosen as optimized time window for behavioral analyses including open field and beam walking tests. At D8, brains were sampled to evaluate CVS, as shown macroscopically in (**C**). (**B**) Surgical procedure of blood injection into the cisterna magna. Blood was collected from carotid artery of a homologous mouse. After animal preparation and installation on stereotactic frame, a nape incision was carried out in the posterior neck, the posterior muscles were separated, and then the underlying muscles were dissected to open an access to the vascularized membrane delimitating the cisterna magna. The pipette was inserted into the cisterna magna before blood injection. (**C**) Illustration of the blood distribution into paravascular spaces twenty-four hours after surgery and of macroscopic CVS after transcardial perfusion of Indian ink five days after surgery in SAH compared with Sham condition. (**D**) Weight

evolution from D-1 to D8 post-surgery in Sham (n=10) and SAH C57Bl/6J (n=15) mice. SAH mice showed a decrease in percentage of body weight gain from D1 to D8 compared with the sham mice ($p<0.01$). ANOVA with Bonferroni's post hoc test for multiple comparison tests. Survival curve following surgery in sham (n=10) and SAH C57Bl/6J (n=15) mice. Data were expressed as Kaplan Meier curves. SAH mice showed a more important mortality at D7 post-surgery compared with sham mice ($p<0.05$). Mantel-Cox test. Please click here to view a larger version of this figure.

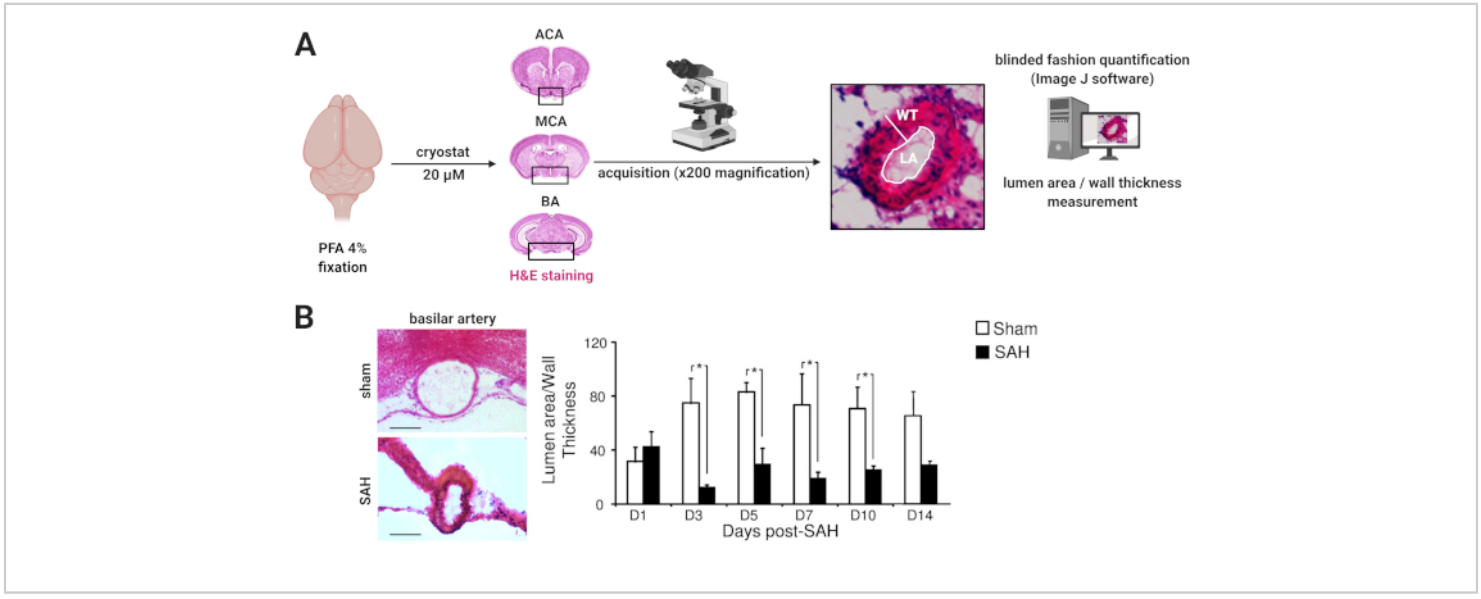

Figure 2. Experimental design for cerebral vasospasm analysis and time course of cerebral vasospasm in basilar artery after SAH. (**A**) Schematic diagram showing the experimental design of protocol for CVS quantification. After post-fixation by 4%PFA, frozen brains were serially sliced using a cryostat into 20 µm transversal slices on gelatin-coated glass slides. Hematoxylin and Eosin (H&E) staining was performed from brain slices bearing ACA, MCA and BA. Microphotographies were acquired using a microscope-mounted camera at a 200x magnification. Lumen area and vessel wall thickness were quantified using ImageJ by a simple blind method. (**B**) Time course of CVS in BA after SAH. Representative microphotographies of H&E staining showing BA morphology (lumen area and wall thickness) in sham and SAH brain slices at D7 post-SAH. Quantification histograms of lumen area/wall thickness ratio showing CVS in the BA from D3 to D10 post-surgery (*, $p<0.05$). Data were expressed as mean ± SEM. n=6/condition. ANOVA with Bonferroni's post hoc test for multiple comparisons. Please click here to view a larger version of this figure.

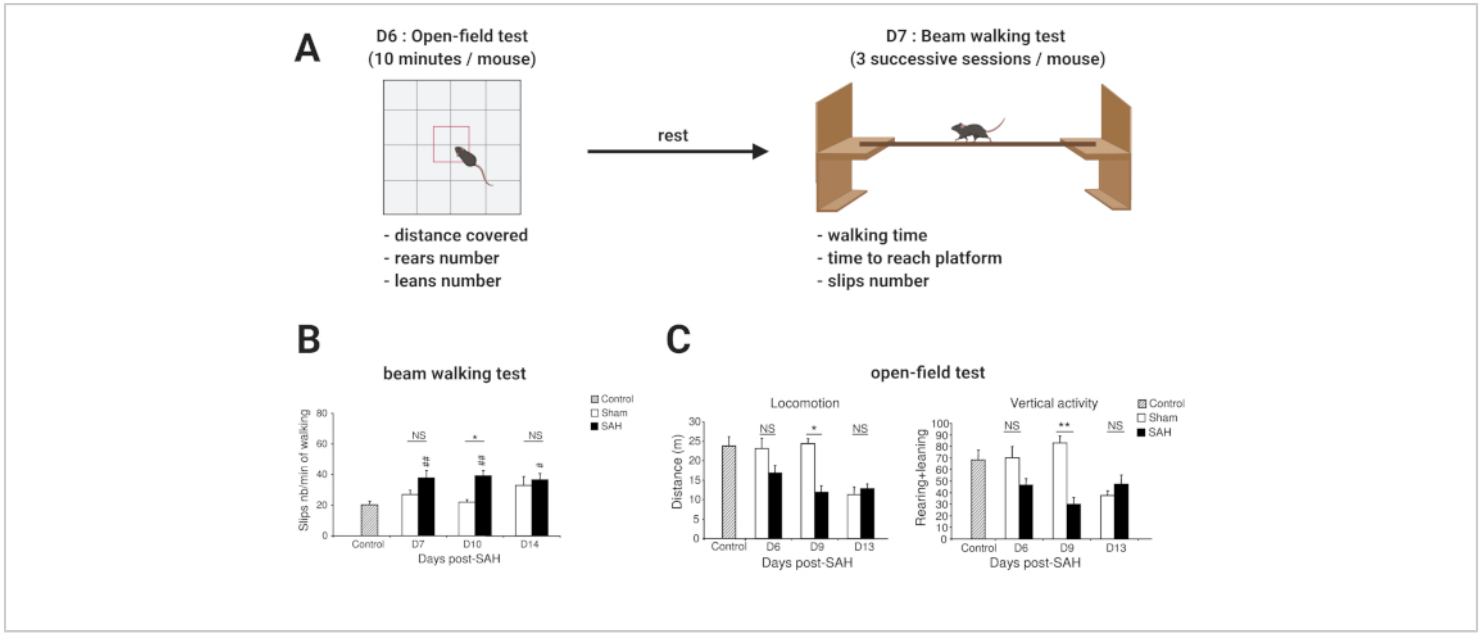

Figure 3. Experimental design for behavioral analysis of long-term sensitivomotor deficits after SAH. (**A**) Schematic diagram showing the experimental design of the behavioral analysis protocol after SAH. Briefly, at D6 post-surgery, motor activity behavior of mice was evaluated by an open-field test for 10 minutes, in which covered distance and the number of rearing and leaning was recorded. After a 24 h rest period, the sensitivomotor behavior of mice was evaluated by the beam walking test, in which the walking time, the time to reach the platform and the number of trips were recorded. (**B**) From El Amki et al.[22] : In the beam walking test, SAH mice showed increased number of trips compared with controls at D7 (**, p<0.01), D10 (***, p<0.001) and D14 (*, p<0.05) and with sham mice at D10 (*, p<0.05). (**C**) From El Amki et al.[22] : SAH mice exhibited a decreased distance crossed (*, p < 0.05) and vertical activity compared with Sham mice at D9 (*, p< 0.01). ANOVA followed by Sidak's multiple comparisons test. Data were expressed as mean ± SEM. n=10-12/condition. Please click here to view a larger version of this figure.

Discussion

Despite the intensity of the research in the field of SAH and the development of therapeutic strategies such as endovascular and pharmacological treatment options increasing over the past twenty years, mortality remains high within the first week of hospital admission and reaches about 50% during the following 6 months[24 , 25] . This current preclinical model by daily double injection of homologous arterial blood into the cisterna magna has been recognized for its validity and its association with a low mortality rate. Indeed, among SAH rodent models, a wide range of mortality rates has been reported: 0-16% mortality with single blood injection into cisterna magn[26 , 27 , 28 , 29 , 30 , 31 , 32 , 33 , 34 , 35] , 10-33% mortality with blood injection into prechiasmatic cister[20 , 27 , 36 , 37] , 16-66% mortality in the model by endovascular perforation[38 , 39 , 40 , 41 , 42 , 43 , 44 , 45] and 0-43% with the model by double blood injection into cisterna magna[34 , 35 , 46 , 47 , 48] . The low mortality rate in the model (9% or 27%, depending on the age of mice) can result from the

weak amount of blood injected, the slow-duration of injection, and the tilting of the animal avoiding localized pressure on the brainstem, compared with other double injection models. In SAH patients, the window of CVS occurrence is classically detected at D4-D10 post-hemorrhage. However, in animals, the time to onset and the duration of CVS are less studied and may vary between HSA models, likely depending on experimental protocols and animal species[21].

In this context, the model here resembles clinical SAH physiopathology in terms of SAH-associated CVS. In general, in endovascular perforation model, CVS occurs in the MCA and BA after 1 hour in rats[40] and after 3 days in mice[17]. In the model by blood injection into prechiasmatic cistern, CVS occurrence was shown between two[49] and eight days[37] in rats. In the model of double injection into cisterna magna in rats, CVS develops between 10 minutes[29] and 3 days[31]. We are the first to describe kinetic of appearance of CVS in a mouse model of SAH by double injection, establishing CVS in main cerebral arteries (ACA, MCA and BA) since 3 days and being sustained until the 10th day post-SAH[22], close to what is observed in SAH patients. This last model could be defined as a skilled model of SAH, severe enough without mortality, allowing investigation of mechanisms and therapeutics targeting CVS.

However, this mouse SAH model may also present some limits. The first point is the lack of vessel wall rupture, as possibly reproduced in the collagenase-induced SAH model, through destruction/digestion of blood vessel basal lamina[50]. As for the occurrence of macroscopic CVS, reduced cerebral blood flow (CBF) in some brain territories is not systematically correlated with neurological outcome, thus CBF should be evaluated in this proposed model of SAH. Previous rat studies using Laser Doppler Flowmetry in a SAH model of double injection demonstrated the CBF acute decrease to 30–52% from baseline after the first injection, with a return to baseline after 2 to 3 days post-injection[51,52,53]. In agreement, it has been shown by MRI a decrease of CBF of 33-50% at D3 and 27–44% at D5 after SAH induction in rat double injection models[54,55]. The double injection into the cisterna magna allows for a predictable distribution of blood along the subarachnoid space, resulting especially in blood clots around the posterior circulation, but can introduce variations in physiological parameters. To avoid intracranial pressure (ICP) from rising with the volume of injected blood entering into the spinal canal, both leading to confounding functional impairments[56], the choice to remove an equivalent volume of cerebrospinal fluid could be done, as previously done in other models[30,51]. In the model here, sham mice received an equivalent volume of aCSF or physiological 0.9% NaCl, depending on the experiment, obviously leading to a rising of ICP. Thus, an acute increase of ICP results in an increase from 18 mmHg to 120 mmHg[27,48,53] in the single injection of blood in the cisterna magna model, from 46 to 107 mmHg[27,37,49] in the prechiasmatic cistern blood injection model, and from 27 to 110 mmHg [39,40,53,57,58] in the endovascular perforation model. In contrast, the double blood injection into cisterna magna was associated with a smaller ICP increase from 60 to 67 mmHg[48,53]. Moreover, the action of removing CSF would also alter ICP and modify CSF. In the SAH model here, the decision was to not remove CSF before blood injection but to accompany surgery by a procedure consisting in hilting the animal head from 30°. The aim is to attenuate ICP by allowing the blood distribution into the anterior circulation, an important and necessary step to mimic human SAH physiopathology. In SAH patients, a sharp rise in ICP is detected and is associated with a transient global cerebral ischemia[59], likely contributing to a sustained impairment of autoregulation and early neuronal cell loss[60].

However, after the first event post-SAH, an early external ventricular drainage is often adopted for concerned SAH patients, to avoid brain swelling and hydrocephalus[61]. Here, the double injection SAH model may not be severe at the first bleeding event to provoke the ICP-dependent consequences observed in patients, but likely reproduce a sustained and mild enhanced ICP for days post-SAH.

In addition, another uncontrolled parameter in the SAH model here was the potential variations of the mean arterial blood pressure (MABP) induced by excessively rapid blood injection procedure[27]. Indeed, MABP typically acutely rises after experimental SAH to preserve cerebral perfusion pressure and thereafter, falls to baseline. In the SAH model here, we injected blood or aCSF (~ 10 µL/min) at a low rate to avoid these MABP variations. Regarding the neurobiological events in this model mimicking those observed in humans, we previously showed that the double blood injection model of SAH induces long-lasting CVS, microthrombosis formation and cerebral brain damage including defect in potential paravascular diffusion from day 3 to day 10 post-SAH[22]. However, recent data describing that CSD is involved in SAH-associated DCI[13] strongly support the pursuit of this type of investigations in the mouse model of double injection. This should enable scientific breakthroughs on the beneficial impact of new therapies targeting CSD.

To conclude, the model of double injection of whole arterial blood into the cisterna magna is a mastered model that allows an easy way to mimic the human SAH physiopathology including CVS, microthrombosis, vascular inflammation, neurological deficits and mortality rate. It represents a validated model for testing novel therapeutic approaches to treat SAH-associated morbi-mortality.

Disclosures

The authors have nothing to disclose.

Acknowledgments

We thank the PRIMACEN platform (Normandie Rouen University, France) for imaging equipment and Mr. Arnaud Arabo, Mrs Julie Maucotel and Mrs Martine Dubois, for animal housing and care. We thank Mrs. Celeste Nicola for lending her voice to the videotaping of the protocol. This work was supported by Seinari Normandy maturation program, Fondation AVC under the aegis of the FRM, Normandie Rouen University and Inserm. The Normandy Region and the European Union (3R project). Europe gets involved in Normandy with European Regional Development Fund (ERDF).

References

1. Rincon, F., Rossenwasser, R. H., Dumont, A. The epidemiology of admissions of nontraumatic subarachnoid hemorrhage in the United States. *Neurosurgery.* **73** (2), 217-222, 212-213 (2013).
2. Sandvei, M. S. et al. Incidence and mortality of aneurysmal subarachnoid hemorrhage in two Norwegian cohorts, 1984-2007. *Neurology.* **77** (20), 1833-1839 (2011).
3. van Gijn, J., Kerr, R. S., Rinkel, G. J. Subarachnoid haemorrhage. *Lancet.* **369** (9558), 306-318 (2007).
4. Solenski, N. J. et al. Medical complications of aneurysmal subarachnoid hemorrhage: a report of the multicenter, cooperative aneurysm study. Participants of the Multicenter Cooperative Aneurysm Study. *Critical Care Medicine.* **23** (6), 1007-1017 (1995).

5. Cahill, J., Calvert, J. W., Zhang, J. H. Mechanisms of early brain injury after subarachnoid hemorrhage. *Journal of Cerebral Blood Flow & Metabolism.* **26** (11), 1341-1353 (2006).
6. Huang, J., van Gelder, J. M. The probability of sudden death from rupture of intracranial aneurysms: a meta-analysis. *Neurosurgery.* **51** (5), 1101-1105; 1105-1107 (2002).
7. Rabinstein, A. A. Secondary brain injury after aneurysmal subarachnoid haemorrhage: more than vasospasm. *Lancet Neurology.* **10** (7), 593-595 (2011).
8. Kivisaari, R. P. et al. MR Imaging After Aneurysmal Subarachnoid Hemorrhage and Surgery: A Long-term Follow-up Study. *American Journal of Neuroradiology.* **22** (6), 1143-1148 (2001).
9. Mayberg, M. R. et al. Guidelines for the management of aneurysmal subarachnoid hemorrhage. A statement for healthcare professionals from a special writing group of the Stroke Council, American Heart Association. *Stroke.* **25** (11), 2315-2328 (1994).
10. Dankbaar, J. W. et al. Relationship between vasospasm, cerebral perfusion, and delayed cerebral ischemia after aneurysmal subarachnoid hemorrhage. *Neuroradiology.* **51** (12), 813-819 (2009).
11. Sehba, F. A., Hou, J., Pluta, R. M., Zhang, J. H. The importance of early brain injury after subarachnoid hemorrhage. *Progress in Neurobiology.* **97** (1), 14-37 (2012).
12. Miller, B. A., Turan, N. et al. Inflammation, vasospasm, and brain injury after subarachnoid hemorrhage. *BioMed Res Int.* **2014**, 384342 (2014).
13. Dreier, J. P. et al. Delayed ischaemic neurological deficits after subarachnoid haemorrhage are associated with clusters of spreading depolarizations. *Brain.* **129** (Pt 12), 3224-3237 (2006).
14. Mayer, S. et al. Global and domain-specific cognitive impairment and outcome after subarachnoid hemorrhage. *Neurology.* **59** (11), 1750-1758 (2002).
15. Al-Khindi, T., Macdonald, R. L., Schweizer, T. A. Cognitive and functional outcome after aneurysmal subarachnoid hemorrhage. *Stroke.* **41** (8), e519-e536 (2010).
16. Macdonald, R. L. et al. Randomized trial of clazosentan in patients with aneurysmal subarachnoid hemorrhage undergoing endovascular coiling. *Stroke.* **43** (6), 1463-1469 (2012).
17. Parra, A. et al. Mouse model of subarachnoid hemorrhage associated cerebral vasospasm: methodological analysis. *Neurological Research.* **24** (5), 510-516 (2002).
18. Schuller, K., Buhler, D., Plesnila, N. A murine model of subarachnoid hemorrhage. *Journal of Visualized Experiments.* (81), e50845 (2013).
19. Lin, C. L. et al. A murine model of subarachnoid hemorrhage-induced cerebral vasospasm. *Journal of Neuroscience Methods.* **123** (1), 89-97 (2003).
20. Sabri, M. et al. Anterior circulation mouse model of subarachnoid hemorrhage. *Brain Research.* **1295**, 179-185 (2009).
21. Leclerc, J. L. et al. A Comparison of Pathophysiology in Humans and Rodent Models of Subarachnoid Hemorrhage. *Frontiers in Molecular Neuroscience.* **11** 71 (2018).

22. El Amki, M. et al. Long-Lasting Cerebral Vasospasm, Microthrombosis, Apoptosis and Paravascular Alterations Associated with Neurological Deficits in a Mouse Model of Subarachnoid Hemorrhage. *Molecular Neurobiology.* **55** (4), 2763-2779 (2018).
23. Clavier, T. et al. Association between vasoactive peptide urotensin II in plasma and cerebral vasospasm after aneurysmal subarachnoid hemorrhage: a potential therapeutic target. *Journal of Neurosurgery.* 1-11 (2018).
24. Kundra, S., Mahendru, V., Gupta, V., Choudhary, A. K. Principles of neuroanesthesia in aneurysmal subarachnoid hemorrhage. *Journal of Anaesthesiology Clinical Pharmacology.* **30** (3), 328-337 (2014).
25. Schertz, M. et al. Incidence and Mortality of Spontaneous Subarachnoid Hemorrhage in Martinique. *PLOS ONE.* **11** (5), e0155945 (2016).
26. Lin, C.-L. et al. A murine model of subarachnoid hemorrhage-induced cerebral vasospasm. *Journal of Neuroscience Methods.* **123** (1), 89-97 (2003).
27. Prunell, G. F., Mathiesen, T., Diemer, N. H., Svendgaard, N.-A. Experimental subarachnoid hemorrhage: subarachnoid blood volume, mortality rate, neuronal death, cerebral blood flow, and perfusion pressure in three different rat models. *Neurosurgery.* **52** (1), 165-176 (2003).
28. Turowski, B. et al. New angiographic measurement tool for analysis of small cerebral vessels: application to a subarachnoid haemorrhage model in the rat. *Neuroradiology.* **49** (2), 129-137 (2007).
29. Boyko, M. et al. The neuro-behavioral profile in rats after subarachnoid hemorrhage. *Brain Research.* **1491**, 109-116 (2013).
30. Muñoz-Sánchez, M. Á. et al. Urotensinergic system genes in experimental subarachnoid hemorrhage. *Medicina Intensiva (English Edition).* **41** (8), 468-474 (2017).
31. Delgado, T., Brismar, J., Svendgaard, N. A. Subarachnoid haemorrhage in the rat: angiography and fluorescence microscopy of the major cerebral arteries. *Stroke.* **16** (4), 595-602 (1985).
32. Solomon, R. A., Antunes, J. L., Chen, R., Bland, L., Chien, S. Decrease in cerebral blood flow in rats after experimental subarachnoid hemorrhage: a new animal model. *Stroke.* **16** (1), 58-64 (1985).
33. Ram, Z., Sahar, A., Hadani, M. Vasospasm due to massive subarachnoid haemorrhage-a rat model. *Acta Neurochirurgica.* **110** (3-4), 181-184 (1991).
34. Glenn, T. C. et al. Subarachnoid hemorrhage induces dynamic changes in regional cerebral metabolism in rats. *Journal of Neurotrauma.* **19** (4), 449-466 (2002).
35. Gules, I., Satoh, M., Clower, B. R., Nanda, A., Zhang, J. H. Comparison of three rat models of cerebral vasospasm. *American Journal of Physiology-Heart and Circulatory Physiology.* **283** (6), H2551-2559 (2002).
36. Sabri, M. et al. Mechanisms of microthrombi formation after experimental subarachnoid hemorrhage. *Neuroscience.* **224**, 26-37 (2012).
37. Jeon, H., Ai, J., Sabri, M., Tariq, A., Macdonald, R. Learning deficits after experimental subarachnoid hemorrhage in rats. *Neuroscience.* **169** (4), 1805-1814 (2010).
38. Silasi, G., Colbourne, F. Long-term assessment of motor and cognitive behaviours in the intraluminal perforation

model of subarachnoid hemorrhage in rats. *Behavioural Brain Researchearch.* **198** (2), 380-387 (2009).

39. Bederson, J. B., Germano, I. M., Guarino, L. Cortical blood flow and cerebral perfusion pressure in a new noncraniotomy model of subarachnoid hemorrhage in the rat. *Stroke.* **26** (6), 1086-1092 (1995).
40. Bederson, J. B. et al. Acute vasoconstriction after subarachnoid hemorrhage. *Neurosurgery.* **42** (2), 352-362 (1998).
41. Park, I.-S. et al. Subarachnoid hemorrhage model in the rat: modification of the endovascular filament model. *Journal of Neuroscience Methods.* **172** (2), 195-200 (2008).
42. Van den Bergh, W. et al. Magnetic resonance imaging in experimental subarachnoid haemorrhage. *Acta Neurochirurgica.* **147** (9), 977-983 (2005).
43. Peng, J. et al. LRP1 activation attenuates white matter injury by modulating microglial polarization through Shc1/PI3K/Akt pathway after subarachnoid hemorrhage in rats. *Redox Biology.* **21**, 101121-101121 (2019).
44. Okada, T. et al. Selective Toll-Like Receptor 4 Antagonists Prevent Acute Blood-Brain Barrier Disruption After Subarachnoid Hemorrhage in Mice. *Molecular Neurobiology.* **56** (2), 976-985 (2019).
45. Tiebosch, I. A. et al. Progression of brain lesions in relation to hyperperfusion from subacute to chronic stages after experimental subarachnoid hemorrhage: a multiparametric MRI study. *Cerebrovascular Diseases.* **36** (3), 167-172 (2013).
46. Weidauer, S., Vatter, H., Dettmann, E., Seifert, V., Zanella, F. E. Assessment of vasospasm in experimental subarachnoid hemorrhage in rats by selective biplane digital subtraction angiography. *Neuroradiology.* **48** (3), 176-181 (2006).
47. Lee, J. Y., Huang, D. L., Keep, R., Sagher, O. Characterization of an improved double hemorrhage rat model for the study of delayed cerebral vasospasm. *Journal of Neuroscience Methods.* **168** (2), 358-366 (2008).
48. Cai, J. et al. A novel intravital method to evaluate cerebral vasospasm in rat models of subarachnoid hemorrhage: a study with synchrotron radiation angiography. *PloS one.* **7** (3), e33366 (2012).
49. Piepgras, A., Thome, C., Schmiedek, P. Characterization of an anterior circulation rat subarachnoid hemorrhage model. *Stroke.* **26** (12), 2347-2352 (1995).
50. Rosenberg, G. A., Mun-Bryce, S., Wesley, M., Kornfeld, M. Collagenase-induced intracerebral hemorrhage in rats. *Stroke.* **21** (5), 801-807 (1990).
51. Raslan, F. et al. A modified double injection model of cisterna magna for the study of delayed cerebral vasospasm following subarachnoid hemorrhage in rats. *Experimental & Translational Stroke Medicine.* **4** (1), 23 (2012).
52. Cai, J. et al. A novel intravital method to evaluate cerebral vasospasm in rat models of subarachnoid hemorrhage: a study with synchrotron radiation angiography. *PLoS One.* **7** (3), e33366 (2012).
53. Lee, J. Y., Sagher, O., Keep, R., Hua, Y., Xi, G. Comparison of experimental rat models of early brain injury after subarachnoid hemorrhage. *Neurosurgery.* **65** (2), 331-343; discussion 343 (2009).
54. Guresir, E. et al. The effect of common carotid artery occlusion on delayed brain tissue damage in the rat

double subarachnoid hemorrhage model. *Acta Neurochir (Wien).* **154** (1), 11-19 (2012).

55. Vatter, H. et al. Time course in the development of cerebral vasospasm after experimental subarachnoid hemorrhage: clinical and neuroradiological assessment of the rat double hemorrhage model. *Neurosurgery.* **58** (6), 1190-1197; 1190-1197 (2006).
56. Leonardo, C. C., Robbins, S., Doré, S. Translating basic science research to clinical application: models and strategies for intracerebral hemorrhage. *Frontiers in Neurology.* **3** 85 (2012).
57. Feiler, S., Friedrich, B., Schöller, K., Thal, S. C., Plesnila, N. Standardized induction of subarachnoid hemorrhage in mice by intracranial pressure monitoring. *Journal of Neuroscience Methods.* **190** (2), 164-170 (2010).
58. Westermaier, T., Jauss, A., Eriskat, J., Kunze, E., Roosen, K. Acute vasoconstriction: decrease and recovery of cerebral blood flow after various intensities of experimental subarachnoid hemorrhage in rats. *Journal of Neurosurgery.* **110** (5), 996-1002 (2009).
59. van Lieshout, J. H. et al. An introduction to the pathophysiology of aneurysmal subarachnoid hemorrhage. *Neurosurgical Review.* **41** (4), 917-930 (2018).
60. Conzen, C. et al. The Acute Phase of Experimental Subarachnoid Hemorrhage: Intracranial Pressure Dynamics and Their Effect on Cerebral Blood Flow and Autoregulation. *Translational Stroke Research.* **10** (5), 566-582 (2019).
61. Connolly, E. S., Jr. et al. Guidelines for the management of aneurysmal subarachnoid hemorrhage: a guideline for healthcare professionals from the American Heart Association/american Stroke Association. *Stroke.* **43** (6), 1711-1737 (2012).